science, engineering and health studies

Research Article

Science, Engineering and Health Studies
https://lio1.tci-thaijo.org/index.php/sehs
ISSN (Online): 2630-0087

Optimization of hydroxypropyl β-cyclodextrin-isophane insulin complex-loaded thiolated chitosan/sodium alginate nanoparticles using full factorial design

Benchawan Chamsai[1], Praneet Opanasopit[2], and Wipada Samprasit[1]*

[1] Department of Pharmaceutical Technology, Collage of Pharmacy, Rangsit University, Pathum Thani 12000, Thailand
[2] Department of Industrial Pharmacy, Faculty of Pharmacy, Silpakorn University, Nakhon Pathom 73000, Thailand

***Corresponding author**:
Wipada Samprasit
wipada.s@rsu.ac.th

***Received**: 4 April 2024*
***Revised**: 14 May 2024*
***Accepted**: 19 May 2024*
***Published**: 5 November 2024*

***Citation**:
Chamsai, B., Opanasopit, P., and Samprasit, W. (2024). Optimization of hydroxypropyl β-cyclodextrin-isophane insulin complex-loaded thiolated chitosan/sodium alginate nanoparticles using full factorial design. Science, Engineering and Health Studies, 18, 24050011.

ABSTRACT

Isophane insulin (N) is challenging to administer orally due to its gastrointestinal instability. Research has shown that partially complexing N with hydroxypropyl β-cyclodextrin (HPβCD-N complexes) enhances its stability. Nanoparticles (NPs) are also frequently used to encapsulate drugs to protect them from degradation. This study aimed to optimize HPβCD-N complex-loaded thiolated chitosan/alginate (TCS/ALG) NPs using a full factorial design. The HPβCD-N complexes were prepared before being loaded into the NPs. Independent variables included the concentrations of TCS, ALG, and HPβCD-N complex, while the dependent variables were particle size and zeta potential. The results demonstrated that TCS and ALG concentrations had a positive and negative effect on particle size, respectively, with smaller particles being favored. The zeta potentials of the NPs increased positively and negatively in proportion to the TCS and ALG concentrations, respectively. The HPβCD-N complexes had a minimal effect on the dependent variables. The NPs made with TCS, ALG, and HPβCD-N complex concentrations of 0.075%, 0.0375%, and 5% w/w, respectively, were the most suitable for achieving small particle size and zeta potential within +30 mV and +50 mV. TEM images showed spherical particles with nanometer diameters. The encapsulated N was found to be approximately 1% w/w, confirming successful loading of N into the NPs. Thus, the optimized formulation shows potential as an NP carriers for N delivery.

Keywords: insulin; nanoparticles; full factorial design; optimization

1. INTRODUCTION

Insulin, a peptide hormone used in diabetes treatment, regulate blood glucose levels by mimicking or enhancing the body's natural insulin production (Rahman et al., 2021). Generally, insulin is administered subcutaneously; however, this method has drawbacks, such as susceptibility to infections, injection-related pain, long-term stress, and a higher risk of hypoglycemia (Zhang et al., 2010; Carino and Mathiowitz, 1999). Therefore, oral

administration is recommended for convenience and improved patient compliance. However, enzyme degradation in the gastrointestinal tract, limited drug stability at gastrointestinal pH, and the physical barrier of the intestinal epithelium—particularly concerning insulin—can impact delivery. Consequently, oral insulin administration should be implemented within a stable environment to ensure that the insulin remains biologically active.

β-cyclodextrin (βCD) is a cyclic oligosaccharide with hydrophobic cavities on the interior and a hydrophilic surface on the exterior. Drug molecules can form complexes with βCD by entering its interior cavities. Insulin has been reported to partially penetrate these cavities in βCD and its derivatives (Sajeesh and Sharma, 2006; Zhang et al., 2010), which help prevent aggregation, thermal denaturation, and degradation. However, βCD's low aqueous solubility limits its pharmaceutical applications. Consequently, derivatives of βCD, such as hydroxypropyl β-cyclodextrin (HPβCD), have been developed and used to overcome this limitation.

Nanoparticles (NPs), with at least one dimension smaller than 1000 nm, are widely used for drug delivery applications, particularly to protect drugs from degradation (Kumari et al., 2010). Polymeric NPs are commonly employed for this purpose. Among the polymers used, chitosan (CS) and sodium alginate (ALG) have been developed for insulin drug delivery (Zhang et al., 2010), with ionic gelation achieved between CS and ALG. The effectiveness of the NPs in drug delivery systems is influenced by factors such as particle size and surface properties, including zeta potential. These properties provide critical information during initial characterization (Kumar and Dixit, 2017). Particle size affects drugs transportation and absorption, as well as NP interactions with cells and tissues (Vinothini and Rajan, 2019). Smaller particles generally allow for higher intracellular absorption compared to microparticles. NPs smaller than 500 nm are absorbed through receptor-mediated endocytosis, while larger NPs are typically taken up via phagocytosis (Vinothini and Rajan, 2019). The surface charge of the NPs, known as zeta potential, measures the difference in potential between the bulk fluid in which the NP is dispersed and the layer of fluid containing oppositely charged ions associated with the NP's surface. This property help assess the physical stability of NPs; a higher magnitude of zeta potential indicates stronger electrostatic repulsion and increased stability (Sharma et al., 2014). NPs with zeta potential values ≤ -30 or ≥ +30 mV generally exhibit high stability (Kumar and Dixit, 2017) and reduced self-aggregation (Wu et al., 2011). Conversely, a low zeta potential may lead to aggregation and flocculation. Therefore, minimizing particle size while maintaining an appropriate zeta potential facilitates the efficient absorption of encapsulated drugs and enhances NPs stability.

The polymers used in the formulations, and the drug concentrations in the reaction mixture affect both particle size and zeta potential (Masalova et al., 2013). The formation of NPs was proportional to the mass ratio of ALG to CS, with insulin primarily encapsulated in the core of the NPs, protecting it from degradation (Zhang et al., 2010). In addition, a mucoadhesive polymer, thiolated triethyl CS, was also developed for insulin-loaded NPs (Rahbarian et al., 2018). The pH and concentration ratio of polymer to insulin also influenced NP characteristics. While our previous research demonstrated the effect of thiolated CS and ALG concentrations on regular insulin-loaded NPs (Chamsai et al., 2023), the composition of each insulin form differed. Isophane insulin (N), which includes protamine in addition to regular insulin, may cause variations in particle size and surface charge of the NPs. Thus, the aim of this research study was to systematically investigate the effects of polymer and N concentrations on the characteristics of HPβCD-N complex-loaded NPs, such as particle size and zeta potential, using a full factorial design. HPβCD-N complexes were produced before being loaded into NPs to enhance the stability of N.

2. MATERIALS AND METHODS

2.1 Materials

Isophane insulin (N) with a dosage of 100 IU/mL was obtained from Novo Nordisk, Bangkok, Thailand. HPβCD with an average molecular weight of 1400 (Cavasol™ W7 HP Pharma) was provided by Ashland Industries Europe GmbH in Schaffhausen, Switzerland. CS with a degree of deacetylation of 0.85 and a molecular weight of 110 kDa, along with alginic acid sodium salt from brown algae (ALG) with low viscosity and an average molecular weight of 30,000–100,000, were received from Sigma, St. Louis, MO, USA. Moreover, 1-Ethyl-3-(3-dimethylaminopropyl) carbodiimide hydrochloride (EDAC), 5,5'-dithio-bis-(2-nitrobenzoic acid) (DTNB), and cysteine hydrochloride were also purchased from Sigma, St. Louis, MO, USA. All other materials and chemicals used were of analytical grade.

2.2 HPβCD-N complexes

The HPβCD-N complexes were prepared following the procedure used in a prior study (Chamsai et al., 2023). In brief, N was dissolved in a solution of diluted hydrochloric acid at pH 3, and the pH was adjusted to 6.8 using 0.1 N NaOH. The N solution was then mixed with an HPβCD solution at a 1:1 weight ratio and agitated slowly on a shaker at 30 rpm for 1 h at 25 °C. The zeta potential of both the N and the HPβCD-N complexes was determined using a Zetasizer Nano ZS (Malvern Instruments, Malvern, UK).

2.3 Thiolated chitosan (TCS)

TCS was synthesized using the methodology described in a previous study (Samprasit et al., 2015). Cysteine hydrochloride in terms of carboxylic acid groups were activated with EDAC before being mixed with the CS solution. This mixture was allowed to react for 6 h within a pH range of 4–5. During synthesis, the carboxylic acid groups of cysteine hydrochloride reacted with the amine groups of TCS, forming amide bonds. After that, the TCS was isolated in the dark through dialysis and then freeze dried under a pressure of 0.05–0.1 bar at -80 °C (Alpha 2–4 LSCbasic, Christ, Germany). The thiol groups in the TCS were quantified spectrophotometrically at 412 nm using Ellman's reagent (DTNB dissolved in 0.1 M phosphate buffer at pH 8 and 1 mM EDTA). The free thiol groups were 470 ± 3 μmol/g of the synthesized TCS.

2.4 Optimization of HPβCD-N complex-loaded TCS/ALG NPs

The HPβCD-N complex-loaded TCS/ALG NPs were produced using the ionotropic gelation process described in a prior study (Chamsai et al., 2023). In brief, HPβCD-N complexes were added into a TCS solution, which was

dissolved in 1% v/v acetic acid. The TCS mixture was then gradually poured into an aqueous ALG solution through a 27 G stainless-steel needle, maintaining a distance of 3.5 cm between the needle and the solution. The mixture was mechanically agitated at 1400 rpm for 30 min. To optimize the formulations, a three-level three-factor full factorial design was employed. This statistical experimental design was carried out using Stat-Ease 360® software (trial version 22.0.4 64-bit, Stat-Ease Inc., Minneapolis, USA). Response surface graphics were used to study the interactions among the variables. The independent factors include the concentrations of TCS (A), ALG (B), and the theoretical content of HPβCD-N complexes (C). The concentration ranges of these variables are shown in Table 1, indicating their low, medium, and high levels. The selected responses were particle size (R_1) and zeta potential (R_2) of the NPs measured by dynamic light scattering (DLS) using a Zetasizer Nano ZS (Malvern Instruments, Malvern, UK). The experimental runs (27) were determined based on the number of independent factors, and the interactions of each factor on NP characteristics were analyzed. Observed responses were correlated using various models, and statistical analysis was performed using ANOVA. Several statistical metrics, including multiple correlation coefficients (R^2), adjusted R^2, and predicted R^2, were computed to determine the best-fitting experimental model. Significance was evaluated by p-values less than 0.05. The response in each trial was modeled using Equation 1, derived from the experimental design of two-factors interactions (2FI):

$$R_i\,(2FI) = b_0 + b_1A + b_2B + b_3C + b_4AB + b_5AC + b_6BC \qquad (1)$$

where R_i represents the response, b_0 is the intercept, and b_i are the linear coefficients (b_1 to b_3) and interaction coefficients (b_4 to b_6). The main effects, A, B, and C, indicate the average value of each factor when varied individually, while AB, AC, and BC are the interaction terms.

Three-dimensional surface plots were used in this study to demonstrate the relationships and interactions between the independent factors and responses. The optimal points were determined using the equation derived from the model, with constraints including a minimum particle size (R_1) and a zeta potential (R_2) of +30 to +50 mV to ensure the long-term stability of NPs.

Table 1. Variables in full factorial design

Independent variables	**Level coded value**		
	Low (-1)	**Medium (0)**	**High (+1)**
A = TCS concentration (% w/v)	0.025	0.050	0.075
B = ALG concentration (% w/v)	0.025	0.050	0.075
C = HPβCD-N complex content (% w/w to polymer)	1	3	5
Dependent variables	**Constraints**		
R_1 = Particle size of NPs (nm)	Minimize		
R_2 = Zeta potential of NPs (mV)	+30 to +50 mV		

2.5 Preparation and evaluation of optimized HPβCD-N complex-loaded TCS/ALG NPs

The optimized TCS/ALG NPs loaded with HPβCD-N complexes were prepared using the previously established method and conditions. Particle size, polydispersity index (PDI), and zeta potential were analyzed in triplicate using a Zetasizer Nano ZS. The average and standard deviation were calculated, and these averages were compared to the predicted values from the experimental design. The relative standard deviation (RSD) was calculated by multiplying the standard deviation by 100 and dividing by the average. To evaluate the effect of HPβCD on NP characteristics, the N-loaded TCS/ALG NPs were prepared and evaluated for particle size, zeta potential and PDI. The morphology of the NPs was determined using transmission electron microscopy (TEM) at an accelerating voltage of 80 kV (Philips, TECNI 20, FEI/Philips Electron Optics, Eindhoven, Netherlands). The average diameter of the optimized NPs was measured using image analysis software (JMicroVision V.1.2.7, Switzerland), based on twenty measurements obtained from the TEM images.

To determine the entrapment efficiency (EE) and capacity (EC) of the N in the NPs, an indirect method was employed. The NPs were centrifuged at 5000 rpm for 30 min at 25 °C using ultracentrifugal filter devices with a molecular weight cutoff (MWCO) of 100 kDa. The supernatant was collected and analyzed for free N content by high-performance liquid chromatography (HPLC, Agilent Technologies Inc., USA). A C18 column (Reprosil-Pur Basic®, Dr. Maisch GmbH, Germany, 250 × 4.6 mm, 5 µm of particle size) was used with an isocratic mobile phase containing of 30% 0.1 M NaH_2PO_4, 35% 0.05 M Na_2SO_4, and 30% acetonitrile, at a flow rate of 1 mL/min and a temperature of 35 °C (Sonaje et al., 2010). The UV-visible detector was set to a wavelength of 214 nm. The EE and EC were calculated using Equations 2 and 3, respectively, as listed below:

$$EE = (N_{total} - N_{free}) / (N_{total}) \times 100\ \% \qquad (2)$$

$$EC = (N_{total} - N_{free}) / (W) \times 100\ \% \qquad (3)$$

where, N_{total} is the total theoretical amount of N added, N_{free} is the amount of N found in the supernatant as determined by HPLC, and W is the total weight of the NPs.

2.6 Statistical analysis

All experimental data was collected at least three times. Data are presented as mean± standard deviation (S.D). A Student's *t*-test was used to determine statistically significant, with a significance level set at $p<0.05$.

3. RESULTS AND DISCUSSION

3.1 Optimization of HPβCD-N complex-loaded TCS/ALG NPs

The HPβCD-N complexes were produced at a 1:1 weight ratio, resulting in four HPβCD molecules, consistent with a

prior study (Bucur et al., 2022). The zeta potential was used to evaluate the surface charge of both N and the HPβCD-N complexes. The surface charge of N was negative (-3.83±0.13 mV), but it became positive (3.06±0.12 mV) in the HPβCD-N complexes. The side chain of N may be included in the hydrophobic cavity of the CDs (Zhang et al., 2010), potentially affect the surface charge. Also, the HPβCD-N complexes might enhance the stability of N by preventing enzyme degradation. The HPβCD-N complex-loaded NPs could further enhance N stability through ionic interactions between negatively charged ALG groups and some positively charged amino groups in TCS. To study the effects of TCS, ALG, and HPβCD-N complexes on NP characteristics, 27 experimental runs were carried out using a full factorial design to optimize the HPβCD-N complex-loaded TCS/ALG NPs. The prepared NPs were characterized for average particle size and zeta potential, as shown in Table 2. The particle sizes varied from nanometers to micrometers, contrasting with our previous study, which reported sizes in the nanometer range for regular insulin-loaded NPs (Chamsai et al., 2023). This difference may be due to the distinct nature of isophane insulin compared to regular insulin. The addition of protamine to regular insulin (Aggarwal et al., 2022) likely influences the particle size of the NPs. The zeta potential values ranged from -18.6.3 to 50.5 mV. Both particle size and zeta potential are crucial for NP interactions with cells and tissues, affecting drug absorption (Vinothini and Rajan, 2019), and stability (Sharma et al., 2014). NPs with a minimum particle size and a zeta potential of ≤ -30 or ≥ +30 mV are considered to have high stability (Kumar and Dixit, 2017). The PDI was also determined during particle size measurement. A PDI value less than 0.3 suggests homogeneous NPs, while a value greater than 0.7 indicates a broad particle size distribution (Danaei et al., 2018). The PDI of all NPs was found to be similar (0.643–0.714, data not shown), indicating a broad size distribution. Thus, PDI was not selected as a dependent criterion for this study, even though minimizing PDI is desirable for achieving a narrow size distribution.

Table 2. The observed responses in the 3^3 full factorial design for HPβCD-N complex-loaded NPs

Run	Independent variables			Dependent variables	
	A:TCS (%w/v)	B:ALG (%w/v)	C:N (%w/w)	Particle size (nm)	Zeta potential (mV)
1	-1	-1	1	23.9±9.7*	3.9±1.6
2	-1	0	1	565±54	-18.6±0.6
3	1	0	1	600±267	32.4±0.2
4	0	-1	-1	550±24	37.5±0.6
5	0	-1	1	640±249	44.3±1.5
6	1	1	-1	27.2±7.3*	-7.9±0.4
7	0	1	-1	18.0±1.0*	-14.2±0.6
8	0	0	1	26.1±16.4*	5.1±0.1
9	0	1	0	18.4±11.6*	-13.8±0.4
10	-1	1	1	208±42	-20.4±0.9
11	0	0	0	506±155	0.6±0.1
12	-1	1	-1	216±73	-21.4±0.6
13	0	1	1	18.5±2.4*	-12.6±0.4
14	-1	-1	0	40.5±4.4*	7.3±0.4
15	-1	-1	-1	48.7±6.8*	-0.5±0.9
16	1	-1	1	361±14	44.0±1.0
17	-1	0	0	179±44	-16.7±0.7
18	-1	1	0	208±3	-20.2±0.4
19	1	0	-1	599±189	35.3±0.9
20	1	1	0	24.8±14.7*	-8.2±0.4
21	0	-1	0	473±28	41.2±1.2
22	-1	0	-1	200±78	-16.5±0.7
23	1	-1	0	450±194	49.8±0.7
24	1	1	1	27.2±8.4*	-8.3±0.1
25	1	0	0	535±13	33.4±0.2
26	0	0	-1	40.8±13.6*	2.7±0.7
27	1	-1	-1	560±45	50.5±0.9

Note: Results present the mean±S.D. (n = 3), *The unit is micrometer (μm).

The data for the observed responses were fitted to various models, and ANOVA was used to estimate the effects of the factors. Significant model terms were identified with p-values < 0.05. The best-fitted model for both particle size and zeta potential was the 2FI model. The equations for particle size and zeta potential in terms of the coded variables are presented as Equations 4 and 5, respectively. The R^2 values of the recommended models for the particle size and zeta potential are shown in Table 3, with close agreement between the predicted and adjusted R^2 values for each response. The statistical measurements for zeta potential were higher compared to those for particle size. Adequate precision, which measures the signal-to-noise ratio and predicts the response based on the associated error, was greater than 4 for both responses, indicating an appropriate model for navigating the design space.

$$\text{Particle size} = 11888.81 - 1799A + 1034.67B - 2144.5C + 15853.5AB + 2017.25AC + 2120.58BC \quad (4)$$

$$\text{Zeta potential} = 7.73 + 18.01A - 22.5B + 0.2389C - 8AB - 1.09AC - 0.2083BC \quad (5)$$

The influence of the factors in the coded equation offers valuable insights into their relative effects. A positive coefficient signifies that an increase in the variable from a low to a high level leads to an increase in the response, whereas a negative coefficient indicates a decrease in the response (Deshmukh and Naik, 2013). For particle size, a negative coefficient suggests that small NPs are favored for optimization, whereas a positive coefficient implies an antagonistic effect (Patel et al., 2015). Specifically, the concentration of TCS was found to positively affect the particle size, resulting in small particles. Conversely, the concentration of ALG and the interaction effects of AB, AC and BC had a negative impacted particle size, leading to larger particles as these variables increased from low to high levels. These findings proved that optimal particles formation occurs when TCS and ALG are present in a stoichiometric proportion (Motwani et al., 2008), facilitating ionic interactions between the positively charged amine groups of TCS and the negative charged carboxylic groups of ALG.

Table 3. Statistical measurements for the recommended model

Statistical measurements	Response	
	Particle size	Zeta potential
R^2	0.7374	0.9330
Adjusted R^2	0.6857	0.9129
Predicted R^2	0.5925	0.8717
Adequate Precision	7.1032	21.6301

Figures 1 and 2 show the three three-dimensional response surface plots for the particle size and zeta potential of the NPs. These plots illustrate the effect of two independent factors on the responses, with the third factor remains constant at its median level. The response surface plots show that the TCS and ALG concentrations had a significant effect on particle size, whereas the HPβCD-N complexes had a slight effect (Figure 1). Furthermore, the zeta potential of the particles was predominantly determined by the TCS and ALG concentrations. These polymers exhibit distinct charges; TCS carries a positive charge due to the protonated $-NH_2$ group, while ALG carries a negative charge due to the -COO groups. As the concentration of TCS increased, the zeta potential became more positive, while an increase in ALG concentration resulted in a more negative zeta potential. In contrast, the concentration of HPβCD-N complexes, had minimal impact on the zeta potential. This stability in zeta potential, even as the content of HPβCD-N complexes was varied (Figure 2), indicates that HPβCD-N complexes can be loaded into the NPs at different concentrations without significantly altering the zeta potential.

The optimal formulation of the HPβCD-N complex-loaded TCS/ALG NPs was chosen to achieve the highest value of the HPβCD-N complexes while minimizing particle size and maintaining the zeta potential within the range of +30 mV to +50 mV (Table 1). The optimal formulation was determined with coded values for factors A, B, and C set at 1, -0.5, and 1, respectively. This resulted in a TCS concentration of 0.075% w/v, an ALG concentration of 0.0375% w/v, and an HPβCD-N complex concentration of 5% w/w. The optimized formulation achieved a predicted particle size of 300.88 nm and a zeta potential of +40.41 mV.

3.2 Characteristics of optimized HPβCD-N complex-loaded TCS/ALG NPs

The optimized formulation of HPβCD-N complex-loaded TCS/ALG NPs was prepared and evaluated for its characteristics. The particle size was within the nanometer range, and the zeta potential was optimal for NP stability (Table 4). The zeta potential values were greater than +30 mV, providing sufficient electrostatic repulsion to prevent self-aggregation and ensure NP stability (Wu et al., 2011). The observed values for the particle size and zeta potential closely matched the predicted values. The relative standard deviation (RSD) value of the predicted errors was low, demonstrating the high predictive accuracy of the response surface methodology used in this study (Deshmukh and Naik, 2013).

Table 4 also shows the characteristics of the N-loaded TCS/ALG NPs compared to the HPβCD-N complex-loaded TCS/ALG NPs, including particle size, zeta potential, and PDI. N-loaded NPs had slightly smaller particle sizes than HPβCD-N complex-loaded NPs, and N-loaded NPs presented a negative zeta potential due to the absence of masking by the HPβCD complexes on the N side chain. These zeta potentials were insufficient to prevent electrostatic repulsion and promote NP stability (Wu et al., 2011). Nonetheless, there was no significant difference in PDI between these two types of NPs. These results revealed that HPβCD affected the NP characteristics, particularly their zeta potential.

TEM analysis was used to assess the shape of the NPs and to verify the results of the particle size measurement, as shown in Figure 3. TEM revealed spherical particles with a diameter of 226.52±19.71 nm. The particle diameter obtained by TEM was smaller than that measured by DLS. This discrepancy may be due to DLS not detecting some aggregated forms of NPs (Raval et al., 2019). Moreover, Danaei et al. (2018) reported that aggregated NPs exhibited a large PDI. The optimized formulation had a PDI of 0.677±0.101, indicating a broad size distribution, possibly due to manual solution dropping. The EE and EC of the N in the NPs were measured using an indirect method, which revealed that the NPs contained 20% of the total amount of added N, with an EC of approximately 1 %w/w (Table 4). This result suggests that not all of the N was fully loaded into the NPs, leaving some in the supernatant of the NP dispersion.

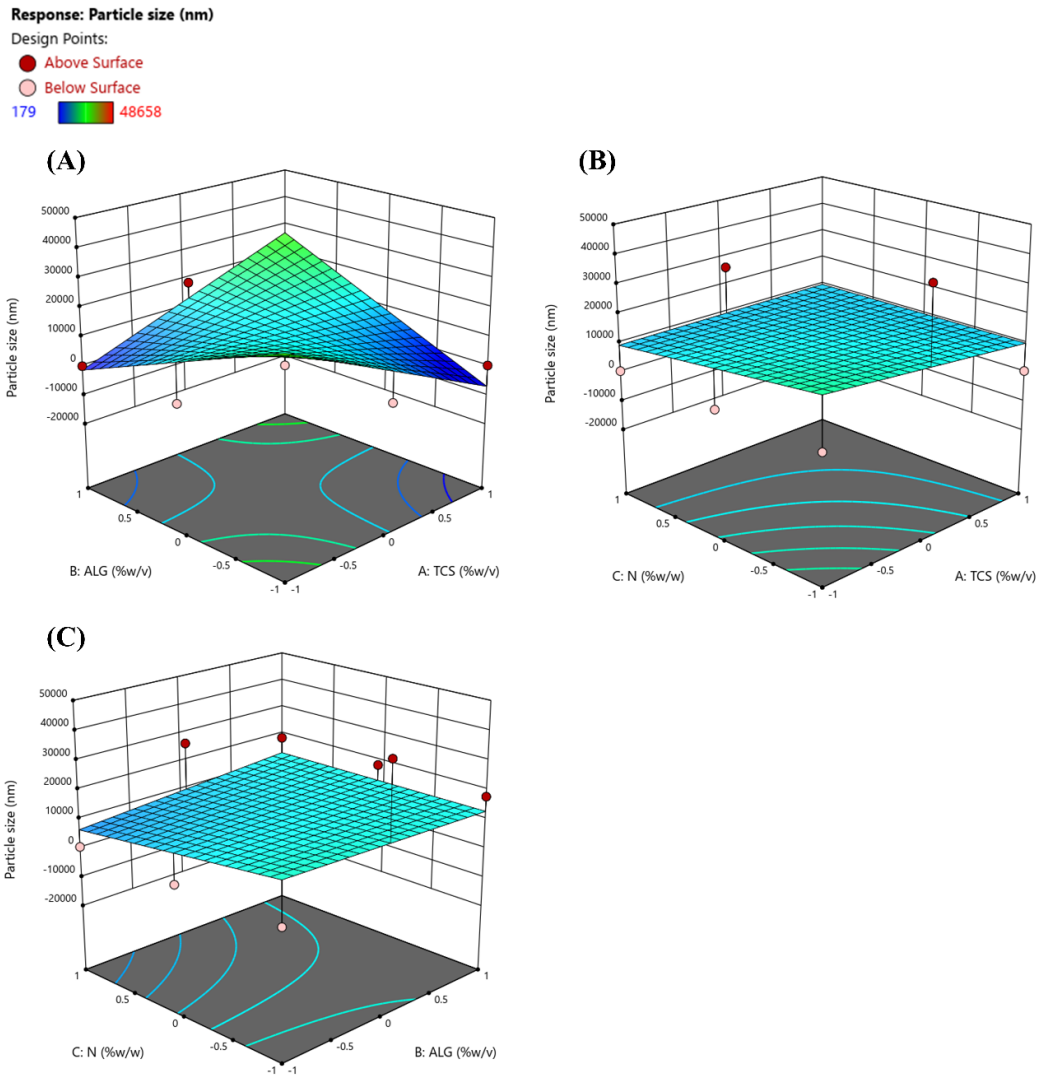

Figure 1. Three-dimensional response surface plots for the response particle size (R_1); (A) any A and B variables taking C at a constant level, (B) A and C variables taking B at a constant level, and (C) B and C variables taking A at a constant level

Table 4. The characteristics of the N-loaded TCS/ALG NPs and the optimized HPβCD-N complex-loaded TCS/ALG NPs based on the predictions obtained by the experimental design and the measurements. Each value shows the mean ± S.D.

Characteristics	**N-loaded NPs**	**HPβCD-N complex-loaded NPs**		
		Predicted value	**Observed value**	**RSD (%)**
Particle size (nm)	297.77±25.98	300.88	333.27±17.43	7.22
Zeta potential (mV)	− 6.55±2.74	+ 40.41	+ 39.10±5.72	2.33
PDI	0.611±0.246	N.D.	0.677±0.101	N.D.
EE (%)	N.D.	N.D.	20.78±2.02	N.D.
EC (%)	N.D.	N.D.	1.04±0.10	N.D.

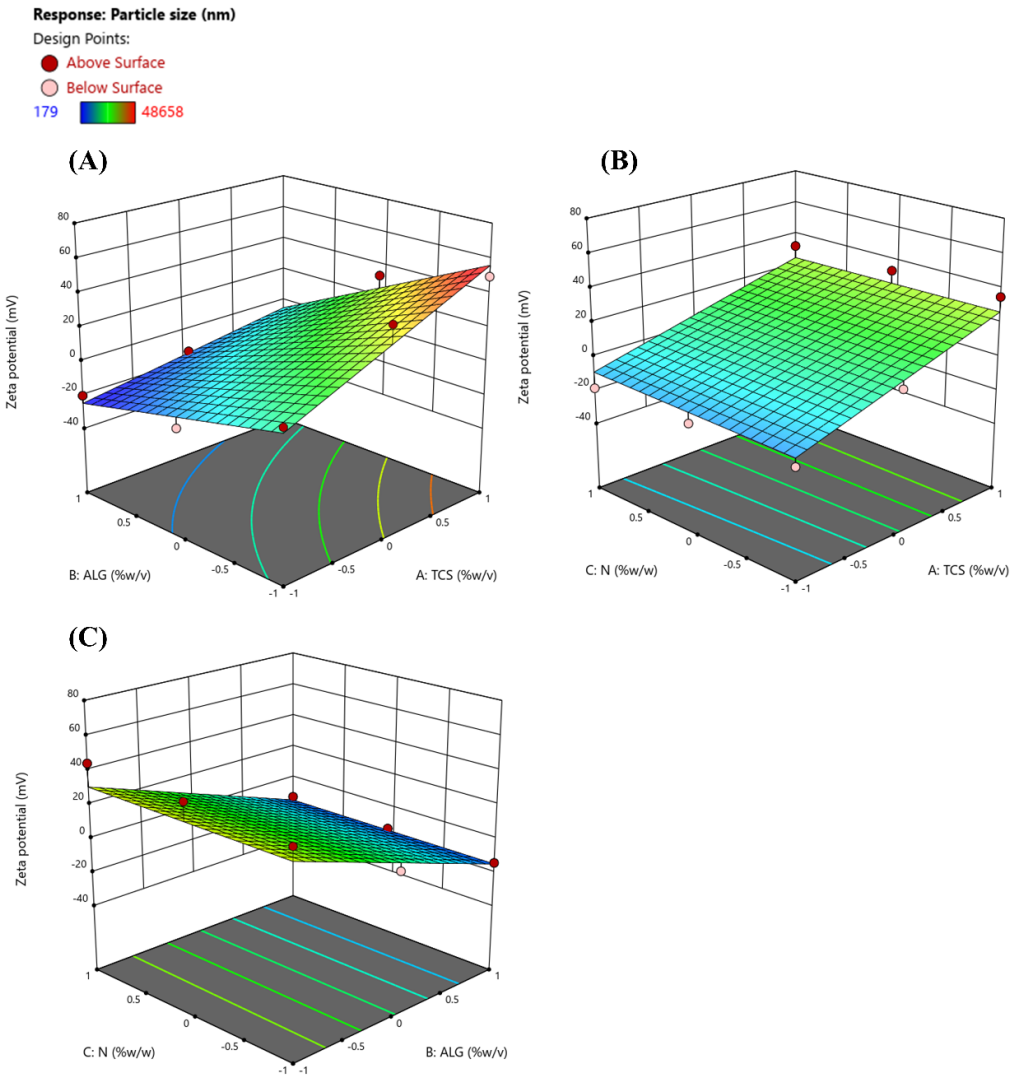

Figure 2. Three-dimensional response surface plots for the response zeta potential (R_2); (A) any A and B variables taking C at a constant level, (B) A and C variables taking B at a constant level, and (C) B and C variables taking A at a constant level

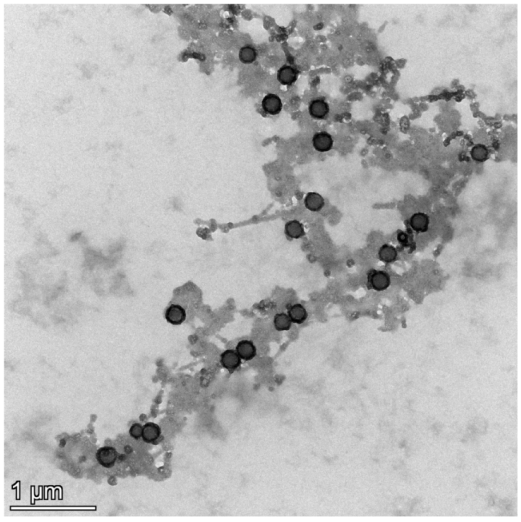

Figure 3. TEM image of the optimized HPβCD-N complex-loaded TCS/ALG NPs

4. CONCLUSION

TCS and ALG are capable of producing NPs suitable for N delivery. The formulation of NPs was optimized using a statistical screening design, with TCS, ALG, and HPβCD-N complex concentrations as the independent variables. The experimental results indicated that TCS and ALG concentrations significantly affected particle size and zeta potential, whereas HPβCD-N complexes had a minor effect. The optimized NP formulation used TCS, ALG and HPβCD-N complexes at concentration of 0.075 %w/v, 0.0375 %w/v and 5 %w/w, respectively. Both predicted and observed responses for particle size and zeta potential of the optimized NPs were within acceptable ranges. TEM images confirmed the spherical nanostructure of the NPs. Furthermore, N loading was approximately 1 %w/w. Thus, the optimized formulation has potential as NP carriers for N delivery. The NPs, along with the HPβCD-N complexes, may increase the stability of the N molecule by preventing enzyme degradation. However, other factors such as pH and temperature also affect NPs and N stability. Further research is required to investigate the structural and conformational changes of N, the release of N from NPs, and the biological activity of N to ensure that the NPs maintain both N stability and activity.

ACKNOWLEDGMENT

This work was funded by the Office of the Permanent Secretary, Ministry of Higher Education, Science, Research and Innovation (OPS MHESI), Thailand Science Research and Innovation (TSRI) (Grant No. RGNS 63–195), the National Research Council of Thailand (NRCT) (Grant No. N42A650551), and Rangsit University.

REFERENCES

Aggarwal, S., Tanwar, N., Singh, A., and Munde, M. (2022). Formation of protamine and Zn-insulin assembly: exploring biophysical consequences. *ACS Omega*, 7(45), 41044–41057.

Bucur, P., Fülöp, I., and Sipos, E. (2022). Insulin complexation with cyclodextrins—A molecular modeling approach. *Molecules*, 27(2), 465.

Carino, G. P., and Mathiowitz, E. (1999). Oral insulin delivery. *Advanced Drug Delivery Reviews*, 35(2–3), 249–257.

Chamsai, B., Opanasopit, P., and Samprasit, W. (2023). Fast disintegrating dosage forms of mucoadhesive-based nanoparticles for oral insulin delivery: Optimization to *in vivo* evaluation. *International Journal of Pharmaceutics*, 647, 123513.

Danaei, M., Dehghankhold, M., Ataei, S., Hasanzadeh Davarani, F., Javanmard, R., Dokhani, A., Khorasani, S., and Mozafari, M. R. (2018). Impact of particle size and polydispersity index on the clinical applications of lipidic nanocarrier systems. *Pharmaceutics*, 10(2), 57.

Deshmukh, R. K., and Naik, B. (2013). Diclofenac sodium-loaded eudragit® microspheres: Optimization using statistical experimental design. *Journal of Pharmaceutical Innovation*, 8, 276–287.

Kumar, A., and Dixit, C. K. (2017). Methods for characterization of nanoparticles. In *Advances in Nanomedicine for the Delivery of Therapeutic Nucleic Acids* (Nimesh, S., Chandra, R., and Gupta, N., Eds.), pp. 43–58. Duxford, Cambridgeshire: Woodhead Publishing.

Kumari, A., Yadav, S. K., and Yadav, S. C. (2010). Biodegradable polymeric nanoparticles based drug delivery systems. *Colloids and Surfaces B: Biointerfaces*, 75(1), 1–18.

Masalova, O., Kulikouskaya, V., Shutava, T., and Agabekov, V. (2013). Alginate and chitosan gel nanoparticles for efficient protein entrapment. *Physics Procedia*, 40, 69–75.

Motwani, S. K., Chopra, S., Talegaonkar, S., Kohli, K., Ahmad, F. J., and Khar, R. K. (2008). Chitosan-sodium alginate nanoparticles as submicroscopic reservoirs for ocular delivery: Formulation, optimisation and *in vitro* characterisation. *European Journal of Pharmaceutics and Biopharmaceutics*, 68(3), 513–525.

Patel, S., Koradia, H., and Parikh, R. (2015). Design and development of intranasal in situ gelling system of Midazolam hydrochloride using 3^2 full factorial design. *Journal of Drug Delivery Science and Technology*, 30(Part A), 154–162.

Rahbarian, M., Mortazavian, E., Dorkoosh, F. A., and Tehrani, M. R. (2018). Preparation, evaluation and optimization of nanoparticles composed of thiolated triethyl chitosan: A potential approach for buccal delivery of insulin. *Journal of Drug Delivery Science and Technology*, 44, 254–263.

Rahman, M. S., Hossain, K. S., Das, S., Kundu, S., Adegoke, E. O., Rahman, M. A., Hannan, M. A., Uddin, M. J., and Pang, M. G. (2021). Role of insulin in health and disease: An update. *International Journal of Molecular Sciences*, 22(12), 6403.

Raval, N., Maheshwari, R., Kalyane, D., Youngren-Ortiz, S. R., Chougule, M. B., Rakesh K., and Tekade, R. K. (2019). Importance of physicochemical characterization of nanoparticles in pharmaceutical product development. In *Basic Fundamentals of Drug Delivery, A volume in Advances in Pharmaceutical Product Development and Research* (Tekade, R. K., Ed.), pp. 369–400. Cambridge, MA: Academic Press.

Sajeesh, S., and Sharma, C. P. (2006). Cyclodextrin-insulin complex encapsulated polymethacrylic acid based nanoparticles for oral insulin delivery. *International Journal of Pharmaceutics*, 325(1–2), 147–154.

Samprasit, W., Kaomongkolgit, R., Sukma, M., Rojanarata, T., Ngawhirunpat, T., and Opanasopit, P. (2015). Mucoadhesive electrospun chitosan-based nanofibre mats for dental caries prevention. *Carbohydrate Polymers*, 117, 933–940.

Sharma, D., Maheshwari, D., Philip, G., Rana, R., Bhatia, S., Singh, M., Gabrani, R., Sharma, S. K., Ali, J., Sharma, R. K., and Dang, S. (2014). Formulation and optimization of polymeric nanoparticles for intranasal delivery of lorazepam using Box-Behnken Design: *In vitro* and *in vivo* evaluation. *BioMed Research International*, 2014(1), 156010.

Sonaje, K., Chen, Y. J., Chen, H. L., Wey, S. P., Juang, J. H., Nguyen, H. N., Hsu, C. W., Lin, K. J., and Sung, H. W. (2010). Enteric-coated capsules filled with freeze-dried chitosan/poly(γ -glutamic acid) nanoparticles for oral insulin delivery. *Biomaterials*, 31(12), 3384–3394.

Vinothini, K., and Rajan, M., (2019). Mechanism for the Nano-Based Drug Delivery System. In *Characterization and Biology of Nanomaterials for Drug Delivery*

(Mohapatra, S. S., Ranjan, S., Dasgupta, N., Mishra, R. K., and Thomas, S., Eds.), pp. 219–263. Amsterdam: Elsevier.

Wu, L., Zhang, J., and Watanabe, W. (2011). Physical and chemical stability of drug nanoparticles. *Advanced Drug Delivery Reviews*, 63(6), 456–469.

Zhang, N., Li, J., Jiang, W., Ren, C., Li, J., Xin, J., and Li, K. (2010). Effective protection and controlled release of insulin by cationic β-cyclodextrin polymers from alginate/chitosan nanoparticles. *International Journal of Pharmaceutics*, 393(1–2), 213–219.